Imaging current flow in lobster nerve cord using the acoustoelectric effect

Russell Witte, Ragnar Olafsson, Sheng-Wen Huang, and Matthew O'Donnell

Citation: Applied Physics Letters **90**, 163902 (2007); doi: 10.1063/1.2724901
View online: http://dx.doi.org/10.1063/1.2724901
View Table of Contents: http://scitation.aip.org/content/aip/journal/apl/90/16?ver=pdfcov
Published by the AIP Publishing

Imaging current flow in lobster nerve cord using the acoustoelectric effect

Russell Witte,[a] Ragnar Olafsson, and Sheng-Wen Huang
Department of Biomedical Engineering, University of Michigan, Ann Arbor, Michigan 48109

Matthew O'Donnell
Department of Bioengineering, University of Washington, Seattle, Washington 98195

(Received 19 February 2007; accepted 15 March 2007; published online 17 April 2007)

Ultrasound traversing a biologic fluid or tissue generates a local change in electrical conductivity known as the acoustoelectric effect. The authors exploit this interaction to image ionic current injected into the abdominal segment of the lobster nerve cord. A pair of recording electrodes detected the acoustoelectric signal induced by pulses of focused ultrasound (1.4 or 7.5 MHz). The signal was linear with injected current at 2 MPa (0.7 μV/mA cm^2) and pressure at 75 mA/cm^2 (23 μV/MPa). Acoustoelectric imaging of biocurrents potentially enhances spatial resolution of traditional electrophysiology and merits further study as an imaging modality for neural applications. © *2007 American Institute of Physics*. [DOI: 10.1063/1.2724901]

Of the 2.5×10^6 people in the United States who suffer from epilepsy, approximately 150 000 are candidates for surgical treatment.[1] Interventional neurosurgery usually requires laborious, pinpoint mapping of cortical function characterized by local field and action potentials to discern eloquent from dormant cortex prior to resection. Although electroencephalogy detects synchronous neural activity from multiple electrodes on the skull, spatial resolution is typically limited to 1 cm or greater. Subdural and penetrating electrodes, on the other hand, substantially improve precision at the cost of invasiveness. In seeking an alternative solution that potentially preserves spatial resolution and minimizes invasiveness of conventional electrical mapping, we exploit an acoustoelectric interaction between local pressure and density to remotely detect current flow in biologic tissue. This imaging approach potentially improves contrast and resolution by constraining the detected signal to where the ultrasound and current wave fields intersect.

The acoustoelectric effect was initially reported by Fox *et al.* in 1946 to characterize colloids in solution.[2] An acoustic pressure wave P traveling in a biologic medium induces a local change in conductivity σ given by

$$(d\sigma)/\sigma = k_1(dP), \tag{1}$$

with k_1 an interaction constant on the order of $0.01\%-0.1\%$/MPa in physiologic saline.[3,4] When P intersects a current field i in a uniform conducting medium, the change in conductivity leads to a voltage modulation V between two recording electrodes of resistance R_0 adjusted by an interaction constant k_2,

$$V(t) = k_2 i R_0 P(t). \tag{2}$$

Consequently, the phase and magnitude of the detected acoustoelectric voltage rely on the ultrasound pressure and applied current as well as the lead fields of the recording electrodes. A more thorough derivation of the signal in an electrolyte solution has been described elsewhere.[3] Recent studies using the acoustoelectric effect have been directed at medicine and biology.[3,5,6] Acoustoelectric tomography, for example, has been proposed for high resolution electrical impedance imaging of breast tissue.[5] We describe a system that measures $V(t)$ in neural tissue that depends on the applied current distribution and location of the ultrasound source. We have previously demonstrated that the sensitivity of acoustoelectric detection in a simulated environment approaches current densities found in the human heart.[7]

A serial three-compartment nerve chamber, traditionally used to stimulate and record from frog and invertebrate tissue, was used to generate and detect the acoustoelectric signal [Fig. 1(a)]. The abdominal segment of a fresh lobster nerve cord was excised and placed in the nerve chamber via a notch in the center divides. The intact nerve extended from the first to the third chamber, each containing lobster Ringer's solution (462 mM NaCl, 16 mM KCl, 26 mM $CaCl_2$, 8 mM $MgCl_2$, 10 mM tris, 10 mM maleic acid, and 11 mM glucose). The middle compartment was sealed with petroleum jelly and filled with mineral oil to electrically isolate the three chambers.

A voltage source (Agilent, Inc. 33120A) and power amplifier (Thorlabs, Inc. model MDT694) were used to generate a 300 Hz sinusoidal current wave form that was injected through a pair of AgCl electrodes placed in chambers 1 and 3. Current levels were monitored with a multimeter and independently verified by sensing the voltage across a 1 Ω resistor placed in series with the electrodes. Current density was estimated from the nerve cross section determined from pulse-echo images. The acoustoelectric signal was captured using a pair of high impedance tungsten recording electrodes placed in the middle chamber. They were separated by 10 mm and touched the exterior of the nerve without penetrating its protective outer sheath. The signals were fed to a differential amplifier (Lecroy, Inc. model 1855A), high pass filter, and second amplifier (Panametrics, Inc. model 5072PR), producing a total gain up to 79 dB. A fast 12 bit data acquisition board (Signatec, Inc. model PDA12) digitized the signal.

The acoustoelectric signal was generated using a dual-element confocal ultrasound transducer (Etalon, Inc.) focused at 50 mm with a 7.5 MHz inner element for imaging and a calibrated 1.4 MHz outer element. The f numbers for the elements were 4 and 2, respectively. The transducer was submerged in de-ionized water. Timing between the current

[a]Electronic mail: ruswit@umich.edu

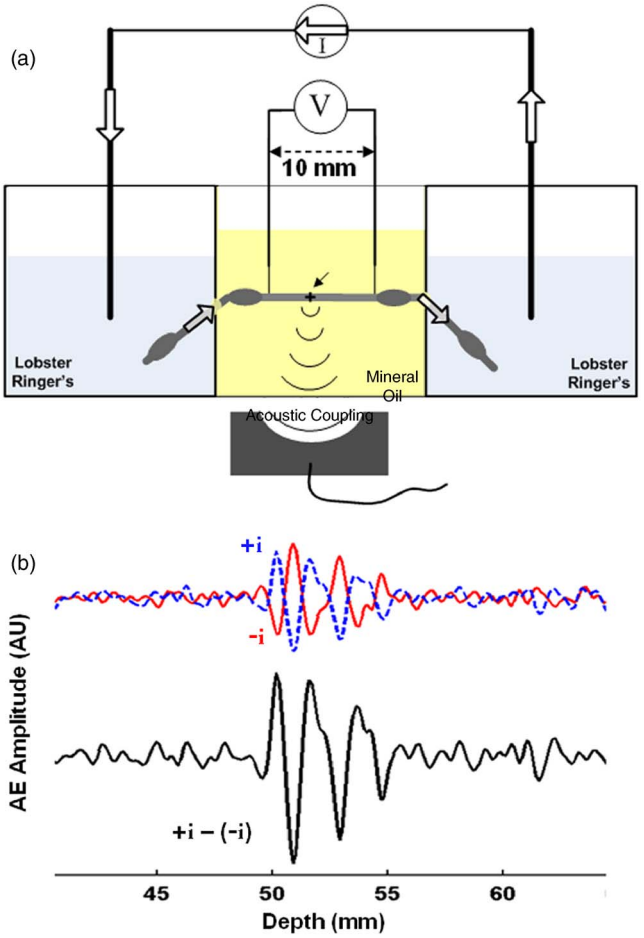

FIG. 1. (Color online) Apparatus for acoustoelectric generation and detection. (a) Abdominal segment of the fresh lobster nerve cord entered all three compartments of the neural chamber. The end compartments contained lobster Ringer's solution. The middle chamber, which contained an acoustic window for passage of ultrasound, was filled with mineral oil to ensure electrical isolation between chambers. A pair of AgCl electrodes in chambers 1 and 3 passed 300 Hz sinusoidal current through the nerve cord, while a second pair of tungsten electrodes detected the acoustoelectric signal. A dual-element confocal ultrasound transducer with center frequencies of 7.5 MHz for the inner element and 1.4 MHz for the outer element provided single pulses at the peak and trough of the injected current wave form. Both pulse-echo and acoustoelectric signals were detected simultaneously. (b) Representative acoustoelectric signals with 7.5 MHz ultrasound focused at the spot denoted by an arrow in (a). The superimposed dashed blue and solid red lines correspond with positive and negative current injections at 80 mA/cm^2, emphasizing the dependence of the acoustoelectric signal on the phase of the current. The subtracted signal depicted underneath demonstrates an improved signal-to-noise ratio due primarily to common mode rejection. Each line was bandpass filtered between 0.2 and 5 MHz.

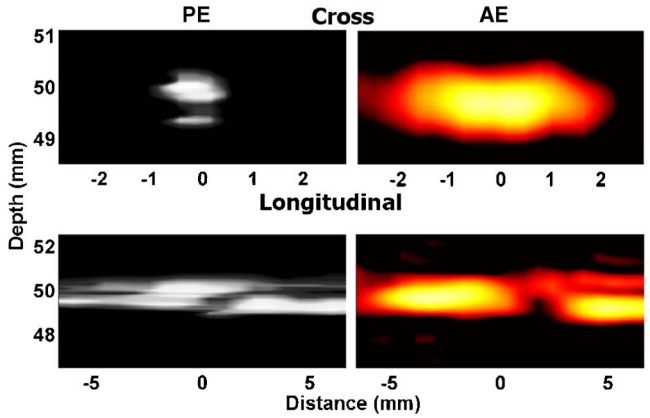

FIG. 2. (Color online) Pulse-echo and acoustoelectric images of lobster nerve cord. Top row: Lateral scan of the ultrasound transducer with an injected current density of 80 mA/cm^2 produced these image cross sections. Pulse-echo (PE) and acoustoelectric (AE) signals were captured simultaneously. The dynamic range of these images is 10 dB. Bandpass filter center frequencies were 7.5 and 2.0 MHz for the pulse-echo and acoustoelectric signals, respectively, reflecting a downshift in the acoustoelectric spectrum. The lateral dimension of current flow through the nerve cord was 4.1 mm (full width at half maximum), which was within the range of the expected value given the downshifted spectrum of the acoustoelectric signal, one-way travel, high f number of 4 of the inner element, and predicted beam pattern of the circular element (Ref. 8) Bottom row: Pulse-echo and acoustoelectric longitudinal sections were obtained by scanning the transducer along the axis of the nerve cord. Dynamic ranges for the pulse-echo and acoustoelectric images are 20 and 25 dB, respectively. Centers of the hot spots of the acoustoelectric image correspond with high sensitivity zones near the recording sites.

source and ultrasound pulse was controlled with a field programmable gate array such that the ultrasound excitation occurred at either the peak or trough of the sinusoidal current wave form. With this approach, the phase of the acoustoelectric signal could be compared to the direction of the current. Subtracting the acoustoelectric signals with positive and negative applied currents also reduced common mode interference and controlled for possible extraneous factors that did not depend on current direction such as the Debye effect.[4,7] Pulse echoes were also recorded simultaneously to provide feedback on nerve position and structure.

Sample acoustoelectric signals are presented in Fig. 1(b) with the 7.5 MHz imaging element focused at the position denoted by the arrow in Fig. 1(a). The superimposed dashed blue and solid red lines correspond with positive and negative current injections of 80 mA/cm^2, respectively, emphasizing the dependence of the acoustoelectric signal on the current phase as well as magnitude. The difference between these signals (Fig. 1(b), bottom) illustrates the improved signal-to-noise ratio due primarily to common mode rejection. The ultrasound transducer was scanned laterally in 0.3 mm steps and along the nerve axis in 0.7 mm steps to produce the pulse-echo and acoustoelectric images in Fig. 2. The spectral peak of the raw acoustoelectric signals was between 1.5 and 2.0 MHz, representing a considerable downshift from the inner element's center frequency of 7.5 MHz. This downshift, which was also observed with simulation, was primarily due to the diameter of the nerve and cylindrical shape of the current field—both of which contributed to the acoustoelectric images. The lateral dimension of current flow through the nerve cord was 4.1 mm based on the full width at half maximum, which was within the range of the expected value, considering the downshifted spectrum, one-way travel, high f number of 4 of the inner element, and predicted beam pattern of the circular element.[8] Finally, the centers of the hot spots in the longitudinal acoustoelectric image (Fig. 2, bottom right) correspond with the approximate location of the recording sites depicted in Fig. 1(a) and were most likely due to the high sensitivity zone of the electrodes coupled with the current and pressure fields.

We also examined the dependence of the peak acoustoelectric amplitude on current density and acoustic pressure. These parameters were systematically varied with 1.4 MHz

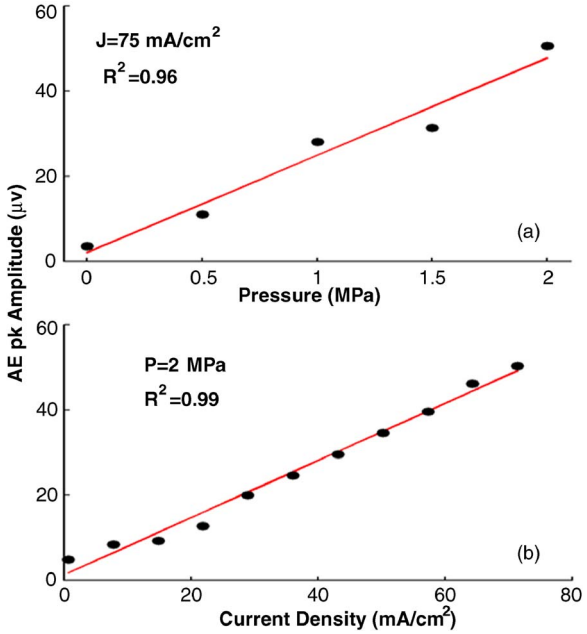

FIG. 3. (Color online) Effect of pressure and current density on peak acoustoelectric signal. Each data point represents the peak differential signal between positive and negative current flow through the lobster nerve cord after 200 averages. The acoustoelectric signal was proportional to (a) incident pressure with a slope of 23 μV/MPa at 75 mA/cm^2 and (b) injected current density with a slope of 0.7 μV/mA cm^2 at 2 MPa. The signal was detected at physiologically relevant current densities less than 10 mA/cm^2 and typical pressures used for clinical ultrasound imaging less than 2 MPa. The acoustoelectric signal at 8 mA/cm^2 was 4 dB above a control signal without current. Current density and pressure are denoted by J and P, respectively.

ultrasound focused on the nerve to determine the sensitivity of the signal (Fig. 3). As predicted by Eq. (2), the acoustoelectric signal was directly proportional to focal pressure with a slope of 23 μV/MPa at 75 mA/cm^2 as well as current density with a slope of 0.7 μV/mA cm^2 at 2 MPa. Both R^2 values were highly significant with $p<0.001$ using Fisher's test. In addition, the signal was detected at physiologically relevant current densities less than 10 mA/cm^2 and at pressures typical for clinical ultrasound imaging. At 8 mA/cm^2 and 2 MPa, for example, the peak magnitude of the acoustoelectric signal was 4 dB above the control signal without current, compared to 23 dB at the highest pressure/current combination depicted in Fig. 3.

Based on the acoustoelectric effect, initial experiments suggest that ultrasound potentially enhances spatial resolution of conventional electrophysiology and may limit the use of invasive, penetrating electrodes during exploratory brain surgery. As predicted from theory, the acoustoelectric signal was proportional to the applied pressure and current density and sensitive to the direction of current flow. Moreover, the acoustoelectric signal was detected at physiologically relevant current densities and moderate acoustic pressures on par with clinical ultrasound imaging. Acoustoelectric imaging of biocurrents potentially impacts a variety of neural applications and merits further study.

This work was supported in part by the National Institutes of Health (EB03451, HL67647, and DE07057).

[1]J. Engel, Jr., Epilepsy Curr. **3**, 37 (2003).
[2]F. Fox, K. Herzfeld, and G. Rock, Phys. Rev. **70**, 329 (1946).
[3]J. Jossinet, B. Lavandier, and D. Cathignol, Ultrasonics **36**, 607 (1998).
[4]J. Jossinet, B. Lavandier, and D. Cathignol, Ann. N.Y. Acad. Sci. **873**, 396 (1999).
[5]H. Zhang and L. Wang, Proc. SPIE **5320**, 145 (2004).
[6]B. Lavandier, J. Jossinet, and D. Cathignol, Ultrasonics **38**, 929 (2000).
[7]R. Olafsson, R. S. Witte, K. Kim, S. Ashkenazi, and M. O'Donnell, Proc. SPIE **6147**, 1 (2006).
[8]X. Chen, K. Q. Schwarz, and K. J. Parker, J. Acoust. Soc. Am. **94**, 2979 (1993).